

Role of occupied d bands in the dynamics of excited electrons and holes in Ag

A. García-Lekue¹, J. M. Pitarke^{1,2}, E. V. Chulkov^{2,3}, A. Liebsch⁴, and P. M. Echenique^{2,3}

¹ *Materia Kondentsatuaren Fisika Saila, Zientzi Fakultatea, Euskal Herriko Unibertsitatea, 644 Posta kutxatila, E-48080 Bilbo, Basque Country*

² *Donostia International Physics Center (DIPC) and Centro Mixto CSIC-UPV/EHU, Manuel de Lardizabal Pasealekua, E-20018 Donostia, Basque Country*

³ *Materialen Fisika Saila, Kimika Fakultatea, Euskal Herriko Unibertsitatea, 1072 Posta kutxatila, E-20080 Donostia, Basque Country*

⁴ *Institut für Festkörperforschung, Forschungszentrum Jülich, 52425 Jülich, Germany*
(Dated: February 6, 2008)

The role that occupied d bands play in the inelastic lifetime of bulk and surface states in Ag is investigated from the knowledge of the quasiparticle self-energy. In the case of bulk electrons, sp bands are taken to be free-electron like. For surface states, the surface band structure of sp states is described with the use of a realistic one-dimensional hamiltonian. The presence of occupied d states is considered in both cases by introducing a polarizable background. We obtain inelastic lifetimes of bulk electrons that are in good agreement with first-principles band-structure calculations. Our surface-state lifetime calculations indicate that the agreement with measured lifetimes of both crystal-induced and image-potential induced surface states on Ag(100) and Ag(111) is considerably improved when the screening of d electrons is taken into account.

PACS numbers: 71.45.Gm, 73.20.At, 73.50.Gr, 78.47.+p

I. INTRODUCTION

Electron scattering in the bulk and at the surface of solid materials has attracted great interest, as the Coulomb interaction between excited electrons and the remaining electrons of the solid is fundamental in many physical and chemical phenomena, such as charge transfer or electronically induced adsorbate reactions at surfaces.^{1,2,3,4} A basic quantity in photoelectron spectroscopy and quantitative surface analysis is the quasiparticle lifetime, which sets the duration of the excitation and combined with the velocity yields the mean free path of the excited state.

Recently, two-photon photoemission (2PPE) and time-resolved 2PPE (TR-2PPE) spectroscopies have provided accurate measurements of the lifetime of both bulk and surface electrons with energies below the vacuum level.^{5,6,7,8,9,10,11,12} The lifetime of bulk and surface holes below the Fermi level has been investigated by employing high-resolution angle-resolved photoemission (ARP) techniques.^{13,14,15,16,17,18,19,20} The scanning tunneling microscope (STM) has also been used to determine the lifetime of both surface-state holes and electrons in the noble metals Cu, Ag, and Au.^{21,22,23,24,25,26}

In the noble metals there are two kinds of surface states: intrinsic surface states of s - p_z symmetry (also called Shockley states)^{27,28,29,30} and image-potential induced surface states.^{31,32,33} Shockley states are localized near the topmost atomic layer and originate in the symmetry breaking at the surface. Image states are Rydberg-like states trapped in the image-potential well outside the surface of a solid with a projected band gap near the vacuum level. Theoretical work based on many-body calculations of the electron self-energy predicted both Shockley and image-state lifetimes that are, in the case

of Cu and other metal surfaces, in good agreement with experiment.^{8,9,10,19,22,34,35,36,37,38,39} The key role that occupied d bands play in the dynamics of image-state electrons has also been investigated,⁴⁰ showing that surface-plasmon decay yields a surprisingly long lifetime of the first image state on the (100) surface of Ag, in agreement with experiment.

In this paper, we report calculations of the inelastic lifetime of both bulk and surface states in Ag, as obtained from the knowledge of the complex quasiparticle self-energy by combining the dynamics of sp valence electrons with a simplified description of the occupied d bands. In the case of bulk electrons, sp bands are taken to be free-electron like. For surface states, single-particle wave functions and energies of sp electrons are taken to be the eigenfunctions and eigenenergies of a realistic one-dimensional hamiltonian that describes the main features of the surface band structure. The dynamically screened electron-electron (e-e) interaction is evaluated within the random-phase approximation (RPA), and the GW approximation of many-body theory is used to compute the complex self-energy. We present the results of calculations of the lifetime of bulk excited electrons with energies below the vacuum level, the first three image states on Ag(100), and both the Shockley and first image state on Ag(111). We find that a realistic description of the screening of d electrons, which reduces the screened e-e interaction and opens (in the case of image states) a new decay channel, is of crucial importance for the understanding of the origin and magnitude of the decay of both bulk and surface states.

Unless stated otherwise, atomic units are used throughout, i.e., $e^2 = \hbar = m_e = 1$.

II. THEORY

In a system of many-electrons, the inverse quasiparticle lifetime is dictated by the imaginary part of the complex energy of the quasiparticle. On the *energy-shell* (i.e., neglecting the quasiparticle-energy renormalization), the lifetime broadening of an excited state $\Phi(\mathbf{r})$ with energy E is given by⁴¹

$$\tau^{-1} = -2 \int d\mathbf{r} \int d\mathbf{r}' \Phi^*(\mathbf{r}) \text{Im} \Sigma(\mathbf{r}, \mathbf{r}'; E) \Phi(\mathbf{r}'). \quad (1)$$

The complex self-energy $\Sigma(\mathbf{r}, \mathbf{r}'; E)$ can be expanded in a perturbative series of the so-called screened interaction $W(\mathbf{r}, \mathbf{r}'; E)$,⁴² which describes the scattering of the excited electron with the remaining electrons of the system. In the GW approximation, one considers only the first-order term in this expansion. If one further replaces the exact one-electron Green function $G(\mathbf{r}, \mathbf{r}', E)$ by its noninteracting counterpart $G^0(\mathbf{r}, \mathbf{r}', E)$, one finds

$$\text{Im} \Sigma(\mathbf{r}, \mathbf{r}'; E) = \sum_f \Phi_f^*(\mathbf{r}') \text{Im} W(\mathbf{r}, \mathbf{r}'; E - E_f) \Phi_f(\mathbf{r}). \quad (2)$$

Here, the sum is extended over all available single-particle states $\Phi_f(\mathbf{r})$ with energy E_f ($E_F \leq E_f \leq E$), E_F is the Fermi energy, and the screened interaction is

$$W(\mathbf{r}, \mathbf{r}'; E) = v(\mathbf{r}, \mathbf{r}') + \int d\mathbf{r}_1 \int d\mathbf{r}_2 v(\mathbf{r}, \mathbf{r}_1) \times \chi(\mathbf{r}_1, \mathbf{r}_2; E) v(\mathbf{r}_2, \mathbf{r}'), \quad (3)$$

where $v(\mathbf{r}, \mathbf{r}')$ represents the bare Coulomb interaction and $\chi(\mathbf{r}, \mathbf{r}'; E)$ is the density-response function of the many-electron system. In the random-phase approximation (RPA),

$$\chi(\mathbf{r}, \mathbf{r}', E) = \chi^0(\mathbf{r}, \mathbf{r}', E) + \int d\mathbf{r}_1 \int d\mathbf{r}_2 \chi^0(\mathbf{r}, \mathbf{r}_1, E) \times v(\mathbf{r}_1, \mathbf{r}_2) \chi(\mathbf{r}_2, \mathbf{r}', E), \quad (4)$$

where $\chi^0(\mathbf{r}, \mathbf{r}', E)$ is the density-response function of non-interacting electrons, which is obtained from a complete set of single-particle wave functions and energies.

A. Bulk states

For a description of the electron dynamics of bulk states in Ag, we consider a homogeneous assembly of interacting valence ($5s^1$) electrons immersed in a polarizable background of d electrons characterized by a local dielectric function $\epsilon_d(\omega)$. Within this model, single-particle wave functions are simply plane waves and the G^0W -RPA (also called G^0W^0) lifetime broadening is obtained from Eqs. (1)-(4) by replacing the bare Coulomb interaction $v(\mathbf{r}, \mathbf{r}')$ by a modified (d -screened) Coulomb interaction $v'(\mathbf{r}, \mathbf{r}'; \omega)$ of the form

$$v'(\mathbf{r}, \mathbf{r}'; \omega) = v(\mathbf{r}, \mathbf{r}') \epsilon_d^{-1}(\omega). \quad (5)$$

By introducing Fourier transforms, the lifetime broadening of an excited bulk state of momentum \mathbf{k} and energy $E = k^2/2$ is then found to be

$$\tau_{\mathbf{k}}^{-1} = -\frac{1}{2\pi^2 k} \int_0^{2k} dq q \int_0^{\omega_{\max}} d\omega \text{Im} W'_q(\omega), \quad (6)$$

where $\omega_{\max} = \min(E - E_F, kq - q^2/2)$, and

$$W'_q(\omega) = \frac{v_q}{\epsilon_q(\omega) + \epsilon_d(\omega) - 1}. \quad (7)$$

Here, $v_q = 4\pi/q^2$, $\epsilon_q(\omega)$ is the RPA dielectric function of valence ($5s^1$) electrons

$$\epsilon_q(\omega) = 1 - v_q \chi_q^0(\omega), \quad (8)$$

$\chi_q^0(\omega)$ being the Fourier transform of the density-response function of non-interacting free electrons, i.e., the Lindhard function.⁴³

In the case of bulk states with energies very close to the Fermi level ($E - E_F \ll E_F$) and in the limit of high electron densities, one finds

$$\tau_E^{-1} = \frac{2(E - E_F)^2}{\pi q_F} \int_0^\infty \frac{dq}{q^4} [q_{TF}^2/q^2 + \epsilon_d(\omega \rightarrow 0)]^{-2}, \quad (9)$$

where q_{TF} is the Thomas-Fermi momentum [$q_{TF} = \sqrt{4q_F/\pi}$] and q_F is the Fermi momentum. The integral entering Eq. (9) is easily carried out to yield

$$\tau_E^{-1} = \frac{(3\pi^2/2)^{1/3}}{36} r_s^{5/2} (E - E_F)^2 / \sqrt{\epsilon_d(\omega \rightarrow 0)}, \quad (10)$$

where r_s is the electron-density parameter⁴⁴ of valence ($5s^1$) electrons.

Eq. (9) shows that the screening of d electrons reduces the lifetime broadening, this reduction being negligible in the long-wavelength ($q \rightarrow 0$) limit where long-range interactions dominate. Eq. (10) shows that the overall impact of d -electron screening is to decrease the lifetime broadening by a factor of $\epsilon_d^{1/2}$, as suggested by Quinn.⁴⁵

B. Surface states

In the case of surface states, interacting valence ($5s^1$) electrons are described by the eigenfunctions and eigenvalues of a realistic one-dimensional hamiltonian that describes the main features of the surface band structure,⁴⁷ and this bounded assembly of valence electrons is then considered to be immersed in a polarizable background of d electrons which extends up to a certain plane $z = z_d$. Within this model there is translational invariance in the plane of the surface, and the G^0W^0 lifetime broadening is obtained from Eqs. (1)-(4), as in the case of bulk states, by replacing the bare Coulomb interaction $v(\mathbf{r}, \mathbf{r}')$ by a modified (d -screened) Coulomb interaction $v'(\mathbf{r}, \mathbf{r}'; \omega)$ whose two-dimensional (2D) Fourier transform

yields (the z axis is taken to be perpendicular from the surface)⁴⁶

$$v'_{\mathbf{q}_{\parallel}}(z, z'; \omega) = \frac{2\pi}{q_{\parallel} \epsilon_d(z', \omega)} [e^{-q_{\parallel}|z-z'|} + \text{sgn}(z_d - z')] \times \sigma_d(\omega) e^{-q_{\parallel}|z-z_d|} e^{-q_{\parallel}|z_d-z'|}, \quad (11)$$

where

$$\epsilon_d(z, \omega) = \begin{cases} \epsilon_d(\omega), & z \leq z_d \\ 1, & z > z_d \end{cases} \quad (12)$$

and

$$\sigma_d = \frac{\epsilon_d(\omega) - 1}{\epsilon_d(\omega) + 1}. \quad (13)$$

The first term in Eq. (11) is simply the bare Coulomb interaction $v_{\mathbf{q}_{\parallel}}(z, z') = 2\pi e^{-q_{\parallel}|z-z'|}/q_{\parallel}$ screened by the polarization charges induced within the polarizable background. The second term stems from polarization charges at the boundary of the medium.

By introducing 2D Fourier transforms, one finds the following expression for the lifetime broadening of an excited state $e^{i\mathbf{k}_{\parallel} \cdot \mathbf{r}_{\parallel}} \phi(z)$ of energy $E = k_{\parallel}^2/(2m) + \varepsilon$:

$$\tau_{\mathbf{k}_{\parallel}, \varepsilon}^{-1} = -2 \int dz \int dz' \phi^*(z) \text{Im} \Sigma_{\mathbf{k}_{\parallel}, \varepsilon}(z, z') \phi(z'), \quad (14)$$

where

$$\text{Im} \Sigma_{\mathbf{k}_{\parallel}, \varepsilon}(z, z') = \sum_{\mathbf{q}_{\parallel}, \varepsilon_f} \phi_f^*(z') \text{Im} W'_{\mathbf{q}_{\parallel}}(z, z'; E - E_f) \phi_f(z), \quad (15)$$

the sum being extended over all available single-particle states $e^{i(\mathbf{k}_{\parallel} - \mathbf{q}_{\parallel}) \cdot \mathbf{r}_{\parallel}} \phi_f(z)$ of energy $E_f = (\mathbf{k}_{\parallel} - \mathbf{q}_{\parallel})^2/(2m_f) + \varepsilon_f$ ($E_f \leq E_f \leq E$). The screened interaction is

$$W'_{\mathbf{q}_{\parallel}}(z, z'; \omega) = v'_{\mathbf{q}_{\parallel}}(z, z'; \omega) + \int dz_1 \int dz_2 v'_{\mathbf{q}_{\parallel}}(z, z_1; \omega) \times \chi_{\mathbf{q}_{\parallel}}(z_1, z_2; \omega) v'_{\mathbf{q}_{\parallel}}(z_2, z'; \omega), \quad (16)$$

where

$$\chi_{\mathbf{q}_{\parallel}}(z, z'; \omega) = \chi_{\mathbf{q}_{\parallel}}^0(z, z'; \omega) + \int dz_1 \int dz_2 \chi_{\mathbf{q}_{\parallel}}^0(z, z_1; \omega) \times v'_{\mathbf{q}_{\parallel}}(z_1, z_2; \omega) \chi_{\mathbf{q}_{\parallel}}(z_2, z'; \omega), \quad (17)$$

and

$$\chi_{\mathbf{q}_{\parallel}}^0(z, z'; \omega) = \frac{2}{A} \sum_{\mathbf{k}_{\parallel}; \varepsilon_i, \varepsilon_j} \phi_i(z) \phi_j^*(z) \phi_j(z') \phi_i^*(z') \times \frac{\theta(E_f - E_i) - \theta(E_f - E_j)}{E_i - E_j + (\omega + i\eta)}, \quad (18)$$

with A being the normalization area, $E_i = \varepsilon_i + k_{\parallel}^2/2$, $E_j = \varepsilon_j + (\mathbf{k}_{\parallel} + \mathbf{q}_{\parallel})^2/2$, $\theta(E)$ the Heaviside function, and η a positive infinitesimal.

We take all the single-particle wave functions and energies entering Eqs. (14)-(18) to be the eigenfunctions and eigenvalues of the one-dimensional hamiltonian of Ref. 47, and we account for the potential variation parallel to the surface through the introduction of the effective masses m and m_f entering the expressions for the total energies E and E_f .

Finally, we note that in the $z_d \rightarrow -\infty$ limit [or, equivalently, if $\epsilon_d(z, \omega)$ is taken to be equal to unity for all z], $v'_{\mathbf{q}_{\parallel}}(z, z'; \omega)$ coincides with the 2D Fourier transform of the bare Coulomb interaction and our lifetime broadening $\tau_{\mathbf{k}_{\parallel}, \varepsilon}$ reduces to that of excited states in the absence of d electrons, as calculated in previous work.^{34,35}

III. RESULTS AND DISCUSSION

A. Bulk states

Silver is a noble metal with $5s^1$ valence electrons and entirely filled $4d$ -like bands. Valence electrons form an electron gas with $r_s = 3.02$. Assuming that the only effect of d electrons is to modify the electron screening of the solid, these electrons are expected to form a polarizable background characterized by a local dielectric function $\epsilon_d(\omega)$ which we take from bulk optical data.⁴⁸ In the static limit ($\omega \rightarrow 0$), $\epsilon_d \sim 4$; in the absence of d electrons, $\epsilon_d(\omega)$ would simply be equal to unity.

Fig. 1 shows the lifetime of bulk excited electrons in Ag versus the electron energy (with respect to the Fermi level), as obtained from Eq. (6) both in the presence (solid line) and in the absence (dashed line) of d electrons. d electrons give rise to additional screening, thus increasing the lifetime of all electrons above the Fermi level. We also compare our results (solid line) with first-principles calculations of the inelastic lifetime of bulk excited electrons in Ag⁴⁹ (solid circles), showing a remarkable agreement for all electron energies under consideration. This indicates that, for excited states within a few eV above the Fermi level, our simplified description of the d bands in Ag [which dominate the density of states (DOS) with energies from ~ 4 eV below the Fermi level] in terms of a polarizable medium is adequate.

In order to analyse the impact of d -electron screening as a function of the momentum transfer, we define the lifetime broadening $\tau_{\mathbf{k}}^{-1}(q_{\max})$ by replacing the actual maximum momentum transfer $2k$ entering Eq. (6) by q_{\max} [which we vary from zero to its actual value $2k$], and consider the ratio

$$r(q_{\max}) = \frac{\int_0^{2q_{\max}} dq q \int_0^{\omega_{\max}} v_q \text{Im} \epsilon_q^{-1}(\omega)}{\int_0^{2q_{\max}} dq q \int_0^{\omega_{\max}} \text{Im} W'_q(\omega)}. \quad (19)$$

We have plotted this ratio in Fig. 2 versus q_{\max} for bulk states with energies very near the Fermi level, showing that in the long-wavelength ($q \rightarrow 0$) limit d electrons do

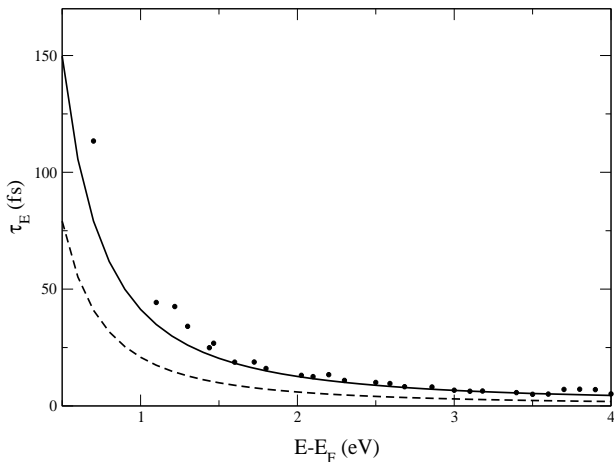


FIG. 1: Lifetime of bulk excited electrons in Ag versus the electron energy (with respect to the Fermi level), as obtained from Eq. (6) both in the presence (solid line) and in the absence (dashed line) of d electrons. Solid circles represent the result of *on-the-energy-shell* first-principles calculations reported in Ref. 49.

not participate in the screening of e-e interactions [see also Eq. (9)]. Hence, if the electron or hole decay were dominated by processes in which the momentum transfer is small, as occurs in the case of Shockley surface states in Ag(111), the overall impact of the screening of d electrons should be expected to be small.

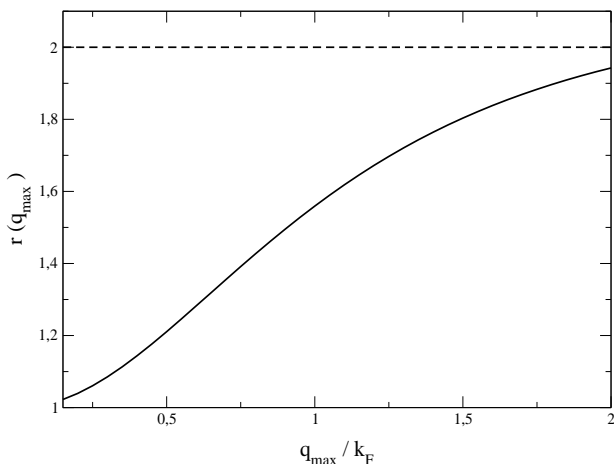


FIG. 2: Ratio $r(q_{\max})$ between the lifetime broadenings $\tau_{\mathbf{k}}^{-1}(q_{\max})$ in the absence [numerator of Eq. (19)] and in the presence [denominator of Eq. (19)] of d bands, as a function of q_{\max} and for bulk states with energies very near the Fermi level ($E - E_F \ll 1$). For these energies, the ratio of Eq. (19), which does not depend on the electron energy E , approaches at $q_{\max} = 2k_F$ the result one would obtain from Eq. (10), i.e., $r(2k) \sim \sqrt{\epsilon_d(\omega \rightarrow 0)} \sim 2$.

B. Surface states

The projected band gaps and available bulk states on the (100) and (111) surfaces of Ag are shown in Fig. 3 at the Γ point ($k_{\parallel} = 0$). In the case of Ag(100), the surface electronic structure supports the whole Rydberg series of image states lying close to the center of the projected band gap. The first three image states have binding energies of 0.53, 0.17, and 0.081 eV ($\epsilon - E = 3.90, 4.26$, and 4.35 eV), and their probability-densities have maxima at 3.8, 14.5, and 32.6 Å outside the crystal edge ($z = 0$), which we choose to be located half a lattice spacing beyond the last atomic layer. In the case of Ag(111), the surface electronic structure supports the first ($n = 1$) image state with a binding energy of 0.77 eV ($\epsilon - E_F = 3.79$), the probability-density being maximum at 0.1 Å inside the crystal edge, and a partially occupied Shockley ($n = 0$) surface state with energy lying at 0.065 eV below the Fermi level and probability maximum at 2.2 Å outside the crystal edge.

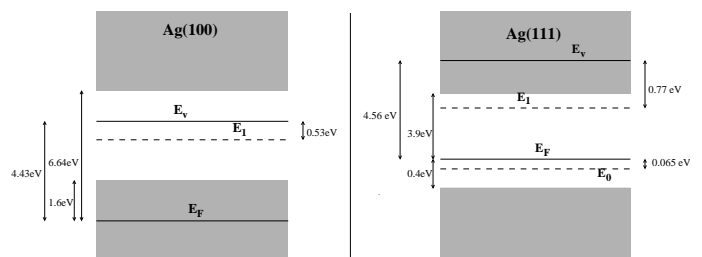


FIG. 3: Projected band gaps and available bulk states on the (100) and (111) surfaces of Ag for $k_{\parallel} = 0$. The shaded area represents the projected bulk bands.

The effective mass of image states is known to be close to the free-electron mass ($m \sim 1$), whereas the effective mass of the $n = 0$ surface state on Ag(111) is found to be $m \sim 0.44$. For all single-particle states below the bottom of the band gap we choose the effective mass to increase from our computed values of 0.45 [Ag(100)] and 0.42 [Ag(111)] at the bottom of the gap to the free-electron mass at the bottom of the valence band. The boundary of the polarizable medium is taken to be at $z_d = -1.5 a_0$ inside the crystal, which was previously found to best reproduce the anomalous dispersion of surface plasmons in Ag.⁵⁰

1. Surface-plasmon excitation

The lifetime broadening of excited states of energy E originates in processes in which the excited electron/hole decays into an empty state above/below the Fermi level. These processes can be realized by transferring energy and momentum to an excitation of the medium, thereby creating either an electron-hole pair or a collective excita-

tion of energy $\omega < |E - E_F|$. Without d -electron screening, the Ag surface-plasmon energy ($\omega_{sp} = 6.5$ eV) is larger than the excitation energies ($|E - E_F|$) under consideration, and only electron-hole pairs can be created. However, the presence of d electrons is known to reduce this surface-plasmon energy from ~ 6.5 to ~ 3.7 eV,⁵⁰ so that relaxation of image states via surface-plasmon excitation becomes feasible and contributes to the lifetime broadening of Eq. (14).

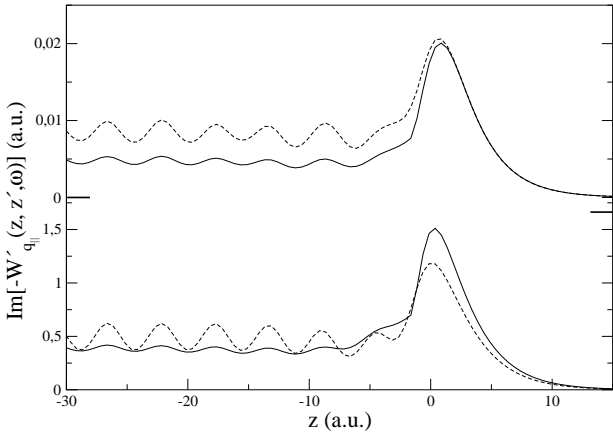


FIG. 4: Imaginary part of the screened interaction $\text{Im}[-W'_{\mathbf{q}_{\parallel}}(z, z'; \omega)]$ versus z for $z' = z$, as obtained from Eq. (16) in the presence (solid lines) and in the absence (dashed lines) of d electrons. The parallel momentum transfer is taken to be $q_{\parallel} = 0.3 q_F$ and two different values are considered for the energy transfer: $\omega = 0.05$ eV (top panel) and $\omega = 4$ eV (bottom panel).

A key ingredient in the decay mechanism of excited states is the imaginary part of the screened interaction $\text{Im}[-W'_{\mathbf{q}_{\parallel}}(z, z'; \omega)]$ entering Eq. (15). Fig. 4 shows this quantity versus the z coordinate both in the presence (solid lines) and in the absence (dashed lines) of d electrons, for $z' = z$, $q_{\parallel} = 0.3 q_F$, and two choices of the energy transfer: $\omega = 0.05$ and 4 eV. d electrons give rise to additional screening; hence, in the interior of the solid they simply reduce $\text{Im}W'$, as in the case of bulk states. However, when the energy transfer approaches the reduced surface-plasmon energy of ~ 3.7 eV (see bottom panel of Fig. 4), this effect is outweighed near the surface by the opening of the surface-plasmon excitation channel which only occurs in the presence of d electrons (solid lines). Hence, while for $\omega = 0.05$ eV the presence of d electrons reduces $\text{Im}[-W']$ both inside the solid and near the surface, for $\omega = 4$ eV d -electron screening enhances $\text{Im}[W']$ near the surface.

Fig. 5 shows the imaginary part of the screened interaction versus the z coordinate, as in Fig. 4, but now for $\omega = 4$ eV and three different values of the momentum

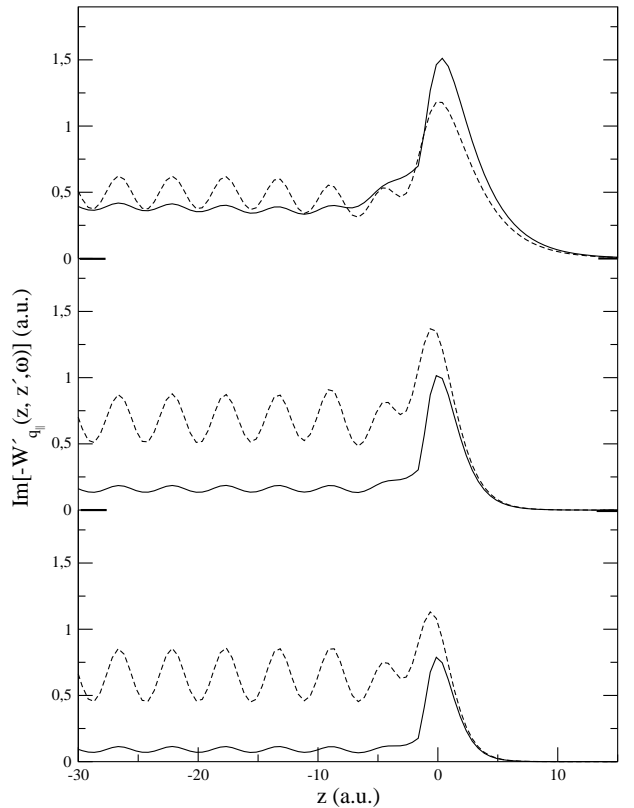


FIG. 5: Imaginary part of the screened interaction $\text{Im}[-W'_{\mathbf{q}_{\parallel}}(z, z'; \omega)]$ versus z for $z' = z$, as obtained from Eq. (16) in the presence (solid lines) and in the absence (dashed lines) of d electrons. Three different values are considered for the parallel momentum transfer: $q_{\parallel} = 0.3 q_F$ (top panel), $q_{\parallel} = 0.6 q_F$ (middle panel), and $q_{\parallel} = 0.8 q_F$ (bottom panel). The energy transfer is taken to be $\omega = 4$ eV.

transfer: $q_{\parallel} = 0.3, 0.6,$ and $0.8 q_F$. For the lowest value of q_{\parallel} (see also Fig. 4) surface plasmons can be excited in the presence of d electrons, which yields an enhancement of $\text{Im}[-W']$ near the surface. As q_{\parallel} increases the impact of d -electron screening is more pronounced in the interior of the solid, as in the case of bulk states, but there is no enhancement of $\text{Im}[-W']$ near the surface, showing that surface-plasmon excitation does not occur for large values of the parallel momentum transfer.

2. Image states on Ag(100)

Now we consider the decay of image states on Ag(100) at the $\bar{\Gamma}$ point. At this point, the energy of the $n = 1$ image state lies 3.9 eV above the Fermi level. Hence, the decay of this excited state can be realized by creating excitations of energy $\omega \leq 3.9$ eV, which in the presence of d electrons can be either electron-hole pairs or surface plasmons.

Calculations of the imaginary part of the Ag(100) $n =$

1 image-state self-energy $\text{Im}[-\Sigma_{\mathbf{k}_{\parallel},\varepsilon}(z, z')]$ entering Eq. (14) were reported in Ref. 40, showing that, as in the case of $\text{Im}[-W']$ (see Figs. 4 and 5), the reduction of the self-energy inside the solid due to the additional screening of d electrons is outweighed near the surface by the opening of the surface-plasmon excitation channel.

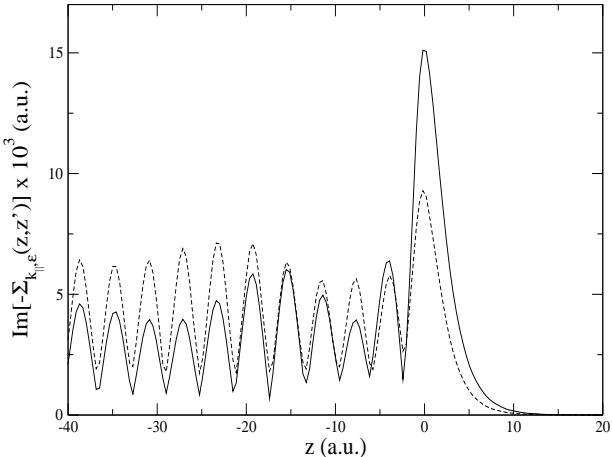


FIG. 6: Maximum of the imaginary part of the $n = 1$ image-state self-energy $\text{Im}[-\Sigma_{\mathbf{k}_{\parallel},\varepsilon}(z, z')]$, versus z , in the vicinity of the (100) surface of Ag, as obtained from Eq. (15) both on the presence (solid lines) and in the absence (dashed lines) of d electrons. For each value of z , $\text{Im}[-\Sigma]$ is evaluated at the z' coordinate for which it is maximum. Inside the solid this occurs at $z' = z$, as in the case of bulk excited states; nevertheless, for z coordinates in the vacuum side of the solid the maximum of $\text{Im}[-\Sigma]$ lags behind and remains localized at $z \sim 0$ rather than $z' = z$, showing a highly nonlocal behaviour in the presence of a metal surface.

The magnitude of the maximum of the imaginary part of the Ag(100) $n = 1$ image-state self-energy is plotted in Fig. 6, as a function of z . This is an oscillating function of z' within the bulk and reaches its highest value near the surface. The oscillatory behaviour within the bulk is dictated by the periodicity of the final-state wave functions $\phi_f(z)$ entering Eq. (15), and the highest value near the crystal edge is the result of the fact that electron-hole pair creation is enhanced in the vicinity of the surface. We note that the presence of d electrons reduces the maximum of $\text{Im}[-\Sigma]$ in the interior of the solid but enhances this quantity near the surface, due to the opening of the surface-plasmon excitation channel. Hence, one might expect from Eq. (14) that this enhancement of $\text{Im}[-\Sigma]$ near the surface should yield an accordingly larger lifetime broadening. The key point of Ref. 40 was, however, to show that this trend is reversed, due to the characteristic non-locality of the self-energy near the surface.

In order to understand this result, we define the lifetime broadening $\tau_{\mathbf{k}_{\parallel},\varepsilon}^{-1}(z_{\max})$ by replacing the upper limit

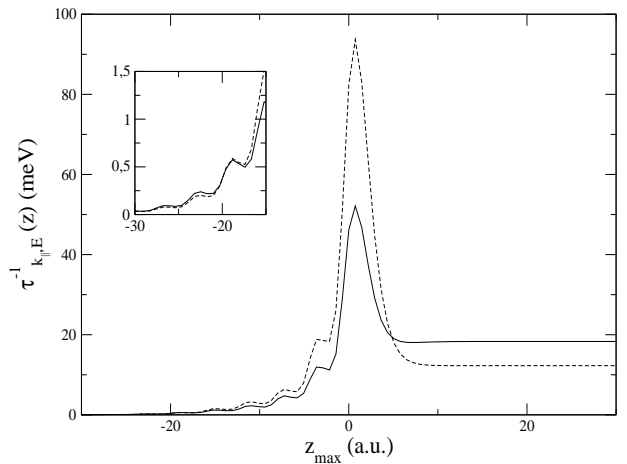


FIG. 7: Lifetime broadening $\tau_{\mathbf{k}_{\parallel},\varepsilon}^{-1}(z_{\max})$ of the $n = 1$ image state at the $\bar{\Gamma}$ point of Ag(100), as obtained from Eq. (14) by replacing the upper limit ($z \rightarrow \infty$) of the integral over z by z_{\max} . Solid and dashed lines represent the result obtained in the presence and in the absence of d electrons, respectively.

($z \rightarrow \infty$) entering the first integral of Eq. (14) by z_{\max} [which we vary from $-\infty$ to its actual value $z_{\max} \rightarrow \infty$]. We have plotted in Fig. 7 the lifetime broadening $\tau_{\mathbf{k}_{\parallel},\varepsilon}^{-1}(z_{\max})$ of the $n = 1$ image state on Ag(100). For z_{\max} well inside the solid (see inset of Fig. 7), coupling of the image state with the crystal only occurs through the penetration of the image-state wave function into the solid, where the presence of d electrons reduce the decay rate. As z_{\max} approaches the surface, coupling of the image state with the crystal is still dominated by the penetration of the image-state wave function into the solid, but now in the presence of d electrons the opening of the surface-plasmon decay channel increases the decay rate. Finally, as z_{\max} moves into the vacuum the imaginary part of the self-energy exhibits a highly nonlocal behaviour (for z outside the solid the main peak of $\text{Im}[-\Sigma]$ lags behind and remains localized at $z \sim 0$), so that coupling mainly occurs through interference between the image-state amplitude at $z > 0$ and the image-state amplitude itself at $z' \sim 0$. Since this amplitude has a node at $z \sim a_0$ (see Ref. 40) and is negative at $z' \sim 0$ where $\text{Im}[-\Sigma]$ is maximum, interference contributions to the lifetime broadening must be negative. As a result, the lifetime broadening $\tau_{\mathbf{k}_{\parallel},\varepsilon}^{-1}(z_{\max})$ is reduced when z_{\max} crosses the surface. Since the presence of d electrons enhances the self-energy near the surface, negative interference is also enhanced and Fig. 7 shows that the net effect of decay via surface plasmons is a considerably reduced lifetime broadening as $z_{\max} \rightarrow \infty$.

We have calculated from Eq. (14) separate contributions to the decay of the first three image states on Ag(100) arising from $z, z' < 0$ ("local" part) and from $z > 0$ or $z' > 0$ ("nonlocal" part), and we have obtained the results presented in Table I. The TR-2PPE measurements reported in Ref. 6 are also presented in this table.

TABLE I: Calculated lifetime broadening $\hbar\tau^{-1}$ (in meV) of the $n = 1, 2$, and 3 image states on Ag(100) either in the presence of a polarizable background of d electrons which extends up to a plane located at $z_d = -1.5a_0$ or in the absence of d electrons ($z_d \rightarrow -\infty$). Local and nonlocal contributions to the lifetime broadening have been obtained by confining the integrals in Eq. (14) to $z, z' < 0$ (local) and by confining these integrals to either $z > 0$ or $z' > 0$ (nonlocal). The experimental linewidth is taken from TR-2PPE experiments.⁶ The lifetime in fs ($1 \text{ fs} = 10^{-15} \text{ s}$) is obtained by noting that $\hbar = 658 \text{ meV fs}$.

n	z_d	Local	Nonlocal	Total	Experiment
1	$-\infty$	34	-16	18	
	-1.5	59	-47	12	12
2	$-\infty$	9	-5	4	
	-1.5	14	-11	3	4
3	$-\infty$	5	-3	2	
	-1.5	6	-5	1	1.8

Our calculations indicate that the impact of d -electron screening on the negative interference near the surface outweighs the increase of the local part of the decay, which yields a reduced lifetime broadening in agreement with experiment.

3. $n = 0$ and $n = 1$ surface states on Ag(111)

Fig. 8 shows the dispersion of the $n = 0$ Shockley state on the (111) surface of Ag. At the $\bar{\Gamma}$ point this is an occupied state; hence, a hole can be created at this point, which will decay through the coupling with bulk states (interband transitions) and through the coupling, within the surface state itself, with surface states of different wave vector parallel to the surface (intraband transitions). Previous calculations of the lifetime broadening of this Shockley hole showed that the broadening arising from intraband transitions represents $\sim 90\%$ of the total decay rate.^{22,37} As the momentum transfer involved in these transitions (see Fig. 8) is very small, the presence of a polarizable medium of d electrons is not expected to play an important role.

The bottom panel of Fig. 9 exhibits the imaginary part of the $n = 0$ Shockley-hole self-energy at the $\bar{\Gamma}$ point both in the presence (solid lines) and in the absence (dashed lines) of d electrons, as a function of z for fixed values of the z' coordinate: $z' = 0$ and $10a_0$. This figure clearly shows that the impact of d -electron screening on the decay of this surface state is nearly negligible. In contrast, the screening of d electrons opens a surface-plasmon decay mechanism for the $n = 1$ image state on Ag(111) (see the top panel of Fig. 9), as occurs in the case of Ag(100).

In Table II we summarize the results we have obtained for the lifetime broadening of both the $n = 0$ and $n = 1$

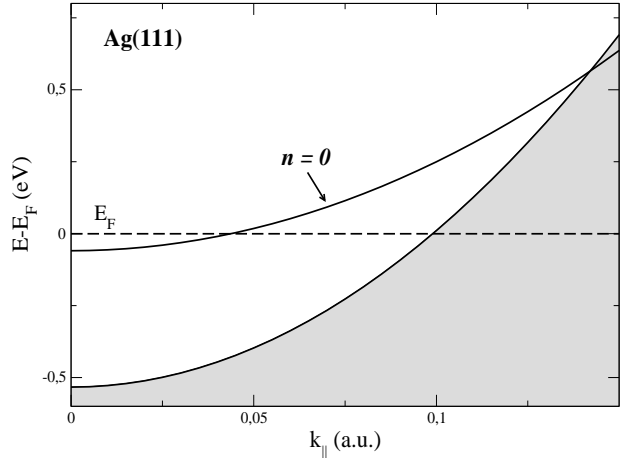


FIG. 8: The solid line represents the dispersion of the Shockley ($n = 0$) surface state on Ag(111). The shaded area represents the projected bulk bands in this surface.

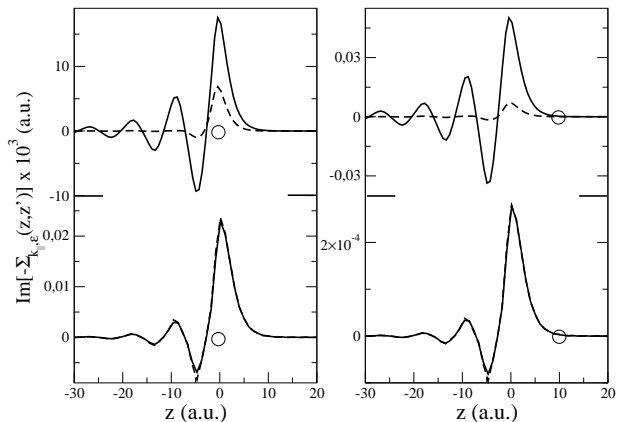


FIG. 9: Imaginary part of the $n = 0$ (bottom panels) and $n = 1$ (top panels) surface-state self-energy $\text{Im}[-\Sigma_{\mathbf{k}_{\parallel}, \epsilon}(z, z')]$ versus z in the vicinity of the (111) surface of Ag, both in the presence (solid lines) and in the absence (dashed lines) of d electrons. The value of the z' coordinate (indicated by an open circle) is fixed at $z' = 0$ (left panels) and $z' = 10a_0$ (right panels). The geometrical electronic edge ($z = 0$) is chosen to be located half an interlayer spacing beyond the last atomic layer. Parallel momentum is taken to be $\mathbf{k}_{\parallel} = 0$. $n = 0$ and $n = 1$ surface-state energies are $\epsilon = E_F + 3.79 \text{ eV}$ and $\epsilon = E_F - 0.065 \text{ eV}$, respectively.

surface states on Ag(111) at the $\bar{\Gamma}$ point. We observe that the broadening is always reduced when d -electron screening participates. The lifetime broadening of the Shockley hole ($n = 0$) is only slightly reduced, because of the weak screening of d electrons involved in the interaction with the Fermi sea. In the case of the $n = 1$ image state, however, both local ($z < 0$ and $z' < 0$) and

nonlocal ($z > 0$ or $z' > 0$) contributions to the broadening are enhanced in the presence of d -electron screening, due to the opening of the surface-plasmon decay channel. Nevertheless, the role that d electrons play enhancing the nonlocal contribution to the decay, which is dominated by negative interference, is more pronounced than the role that these electrons play enhancing the local decay. As a result, the net effect of decay via surface plasmons is a considerably reduced lifetime broadening, as occurs in the case of image states on Ag(100).

TABLE II: Calculated lifetime broadening $\hbar\tau^{-1}$ (in meV) of the Shockley ($n = 0$) and image ($n = 1$) surface states on Ag(111) either in the presence of a polarizable background of d electrons which extends up to a plane located at $z_d = -1.5 a_0$ or in the absence of d electrons ($z_d \rightarrow -\infty$). Local and nonlocal contributions to the lifetime broadening have been obtained by confining the integrals in Eq. (14) to $z, z' < 0$ (local) and by confining these integrals to either $z > 0$ or $z' > 0$ (nonlocal). The experimental linewidths of Shockley and image states are taken from Refs. 22 and 6, respectively. The lifetime in fs ($1 \text{ fs} = 10^{-15} \text{ s}$) is obtained by noting that $\hbar = 658 \text{ meV fs}$.

n	z_d	Local	Nonlocal	Total	Experiment
0	$-\infty$	1	2	3	
	-1.5	1	1.8	2.8	6
1	$-\infty$	48	-4	44	
	-1.5	103	-67	36	22

Also shown in Table II are low-temperature STM measurements²² of the lifetime of an excited hole at the edge ($\bar{\Gamma}$ point) of the partially occupied $n = 0$ surface state and the 2PPE measurements reported by McNeill *et al.* for the $n = 1$ image state,⁵ both on the (111) surface of Ag. At this point, we note that electron-phonon scattering is expected to yield a contribution to the $n = 0$ surface-state linewidth of 3.9 meV,³⁹ which would result in a total linewidth of 6.7 meV in good agreement with the experimentally measured linewidth of 6 meV. On the other hand, our calculations show that the inclusion of the surface-plasmon decay channel leads to a better agreement of the calculated $n = 1$ image-state linewidth with experiment, although our calculated linewidth for this surface state is still too high.

IV. SUMMARY AND CONCLUSIONS

We have investigated the role that occupied d bands play in the lifetime of bulk and surface states in Ag, by combining an accurate description of the dynamics of sp valence electrons with a physically motivated model in which the occupied d bands are accounted for by the

presence of a polarizable medium. In the case of bulk excited states, we have obtained lifetimes that are in good agreement with first-principles band-structure calculations. Our surface-state lifetime calculations indicate that the agreement with measured lifetimes of both the $n = 0$ crystal-induced and the lowest-lying $n = 1$ image-potential induced surface states on silver surfaces is considerably improved when the screening of d electrons is taken into account.

The impact of d -electron screening on the dynamics of the Shockley surface hole on Ag(111) is entirely due to the reduction of the screened interaction between the excited hole and the Fermi sea. Since the decay of the excited hole is dominated by intraband transitions within the Shockley surface band itself, where the parallel momentum transfer is always very small, the screening of d electrons is comparatively weak and the lifetime broadening is reduced by no more than 10%.

As far as image states are concerned, the reduction (in the presence of d electrons) of the surface-plasmon energy from 6.5 to 3.7 eV opens a new decay channel that enhances the image-state self-energy and more than compensates the reduction of the screened e-e interaction. Nevertheless, our results demonstrate that the highly nonlocal character of the self-energy near the surface ultimately leads to a reduced lifetime broadening of image states on both the (100) and (111) surfaces of Ag. In the case of the $n = 1$ image state on Ag(100), the reduced lifetime broadening is in excellent agreement with the experiment. The agreement with the measured lifetime of the $n = 1$ image state on Ag(111) is also improved when the screening of d electrons is considered, although in this case the experimental linewidth is still well above the theoretical prediction. The experimental linewidths of the $n = 2$ and $n = 3$ image states on Ag(100) are also slightly above our best theoretical prediction, as occurs in the case of the corresponding image states on Cu(100).³⁵ As the linewidth of excited image states ($n > 1$) is only of a few meV's, small discrepancies with the experiment may be attributed to a combination of scattering with phonons, many-body effects beyond the *GW* approximation, and the necessity of an *ab initio* description of the dynamical response of both sp and d electrons in the noble metals.

Acknowledgments

We acknowledge partial support by the University of the Basque Country, the Basque Unibertsitate eta Ik-erketa Saila, the Spanish Ministerio de Ciencia y Tecnología, and the Max Planck Research Award Funds.

¹ N. H. Ge, C. M. Wong, R. L. Lingle, J. D. McNeill, K. J. Gaffney, and C. B. Harris, *Science* **279**, 202 (1998).

² M. Wolf and G. Ertl, *Science* **288**, 1352 (2000).

³ H. Petek, M. J. Weida, H. Nagano, and S. Ogawa, *Science*

- 288**, 1402 (2000).
- ⁴ H. Nienhaus, Surf. Sci. Rep. **45**, 1 (2002).
 - ⁵ J. D. McNeill, R. L. Lingle, N. H. Ge, C. M. Wong, R. E. Jordan, and C. B. Harris, Phys. Rev. Lett. **79**, 4646 (1997).
 - ⁶ U. Höfer, I. L. Shumay, C. Reuss, U. Thomann, W. Wallauer, and T. Fauster, Science **277**, 1480 (1997); L. Shumay, U. Höfer, U. Thomann, W. Wallauer, and T. Fauster, Phys. Rev. B **58**, 13974 (1998).
 - ⁷ E. Knoesel, A. Hotzel, and M. Wolf, J. Electron Spectrosc. Relat. Phenom. **88-91**, 577 (1998).
 - ⁸ A. Schäfer, I. L. Shumay, M. Wiets, M. Weinelt, T. Fauster, E. V. Chulkov, V. M. Silkin, and P. M. Echenique, Phys. Rev. B **61**, 13159 (2000).
 - ⁹ S. Link, H. A. Durr, G. Bihlmayer, S. Blugel, W. Eberhardt, E. V. Chulkov, V. M. Silkin, and P. M. Echenique, Phys. Rev. B **63**, 115420 (2001).
 - ¹⁰ W. Berthold, U. Hofer, P. Feulner, E. V. Chulkov, V. M. Silkin, and P. M. Echenique, Phys. Rev. Lett. **88**, 56805 (2002).
 - ¹¹ M. Roth, M. T. Pickel, J. X. Wang, M. Weinelt, and T. Fauster, Phys. Rev. Lett. **88**, 96802 (2002).
 - ¹² X. J. Shen, H. Kawak, A. M. Radojevic, S. Smadici, D. Mocuta, and R. M. Osgood, Chem. Phys. Lett. **351**, 1 (2002).
 - ¹³ B. A. McDougall, T. Balasubramanian, and E. Jensen, Phys. Rev. B **51**, 13891 (1995); F. Theilmann, R. Matzdorf, G. Meister, and A. Goldmann, Phys. Rev. B **56**, 3632 (1997).
 - ¹⁴ M. Hensberger, D. Purdie, P. Segovia, M. Garnier, and Y. Baer, Phys. Rev. Lett. **83**, 592 (1999); M. Hensberger, R. Frésard, P. Purdie, P. Segovia, and Y. Baer, Phys. Rev. B **60**, 10796 (1999).
 - ¹⁵ T. Valla, A. V. Fedorov, P. D. Johnson, and S. L. Hulbert, Phys. Rev. Lett. **83**, 2085 (1999).
 - ¹⁶ P. Straube, F. Pforte, T. Michalke, K. Berge, A. Gerlach, and A. Goldmann, Phys. Rev. B **61**, 14072 (2000).
 - ¹⁷ A. Gerlach, K. Berge, A. Goldmann, I. Campillo, A. Rubio, J. M. Pitarke, and P. M. Echenique, Phys. Rev. B **64** 85423 (2001).
 - ¹⁸ F. Reinert, G. Nicolay, S. Schmidt, D. Ehm, and S. Hüfner, Phys. Rev. B **63**, 115415 (2001).
 - ¹⁹ T. Balasubramanian, L. I. Johansson, P. -A. Glans, C. Virojanadara, V. M. Silkin, E. V. Chulkov, and P. M. Echenique, Phys. Rev. B **64**, 205401 (2001); V. M. Silkin, T. Balasubramanian, E. V. Chulkov, A. Rubio, and P. M. Echenique, Phys. Rev. B **64**, 085334 (2001).
 - ²⁰ S. T. Tang, Ismail, P. T. Sprunger, and E. W. Plummer, Phys. Rev. B **65**, 235428 (2002).
 - ²¹ L. Burgi, O. Jeandupeux, H. Brune, and K. Kern, Phys. Rev. Lett. **82**, 4516 (1999).
 - ²² J. Kliewer, R. Berndt, E. V. Chulkov, V. M. Silkin, P. M. Echenique, and S. Crampin, Science **288**, 1399 (2000).
 - ²³ H. Hövel, B. Grimm, and B. Reihl, Surf. Sci. **477**, 43 (2001).
 - ²⁴ V. Yu. Yurov, A. Bendounan, B. Kierren, Y. F. Revurat, E. Bertran, and D. Malterre, Phys. Low-Dim. Struct., **11/12**, 155 (2001).
 - ²⁵ L. Vitali, P. Wahl, M. A. Schneider, K. Kern, V. M. Silkin, E. V. Chulkov, and P. M. Echenique, Surf. Sci. **523**, L47 (2003).
 - ²⁶ M. Pivetta, F. Silly, F. Patthey, J. P. Pelz, and W.-D. Schneider, Phys. Rev. B. (in press).
 - ²⁷ W. Shockley, Phys. Rev. **56**, 317 (1939).
 - ²⁸ P. O. Gartland and B. J. Slagsvold, Phys. Rev. B **12**, 4047 (1975).
 - ²⁹ W. Eberhardt and E. W. Plummer, Phys. Rev. B **21**, 3245 (1980).
 - ³⁰ F. J. Himpsel, Comments Cond. Mat. Phys. **12**, 199 (1986).
 - ³¹ P. M. Echenique and J. B. Pendry, J. Phys. C **11**, 2065 (1978).
 - ³² N. V. Smith, Rep. Prog. Phys. **51**, 1227 (1988).
 - ³³ P. M. Echenique, J. M. Pitarke, E. V. Chulkov, and V. M. Silkin, J. Electron Spectrosc. **126**, 163 (2002).
 - ³⁴ E. V. Chulkov, I. Sarria, V. M. Silkin, J. M. Pitarke, and P. M. Echenique, Phys. Rev. Lett. **80**, 4947 (1998); J. Osma, I. Sarria, E. V. Chulkov, J. M. Pitarke, and P. M. Echenique, Phys. Rev. B **59**, 10591 (1999).
 - ³⁵ I. Sarria, J. Osma, E. V. Chulkov, J. M. Pitarke, and P. M. Echenique, Phys. Rev. B **60**, 11795 (1999).
 - ³⁶ E. V. Chulkov, V. M. Silkin, and P. M. Echenique, Surf. Sci. **454-456**, 458 (2000); V. M. Silkin and E. V. Chulkov, Phys. Solid State **42**, 1373 (2000) [translated from Fiz. Tverd. Tela **42**, 1334 (2000)].
 - ³⁷ P. M. Echenique, J. Osma, V. M. Silkin, E. V. Chulkov, and J. M. Pitarke, Appl. Phys. A **71**, 503 (2000); P. M. Echenique, J. Osma, M. Machado, V. M. Silkin, E. V. Chulkov, and J. M. Pitarke, Prog. Surf. Sci. **67**, 271 (2001).
 - ³⁸ A. Fukui, H. Kasai, and A. Okiji, Surf. Sci. **493**, 671 (2001); A. Fukui, H. Kasai, H. Nakanishi, and A. Okiji, J. Phys. Soc. Jpn. **70**, 29 (2001).
 - ³⁹ A. Eiguren, B. Ellsing, F. Reinert, G. Nicolay, E. V. Chulkov, V. M. Silkin, S. Hüfner, and P. M. Echenique, Phys. Rev. Lett. **88**, 66805 (2002).
 - ⁴⁰ A. Garcia-Lekue, J. M. Pitarke, E. V. Chulkov, A. Liebsch, and P. M. Echenique, Phys. Rev. Lett. **89**, 096401 (2002).
 - ⁴¹ P. M. Echenique, J. M. Pitarke, E. V. Chulkov, and A. Rubio, Chem. Phys. **251**, 1 (2000).
 - ⁴² A. L. Fetter y J. D. Wallecka, *Quantum theory of Many Particle Systems*, (MacGraw-Hill, New York, 1964).
 - ⁴³ J. Lindhard, K. Dan. Vidensk. Selsk. Mat.-Fys. Medd. **28** (8), 1 (1954).
 - ⁴⁴ r_s is defined as $(4\pi/3)(r_s a_0)^3 = 1/n$, n being the electron density and a_0 the Bohr radius [$a_0 = 0.529 \text{ \AA}$].
 - ⁴⁵ J. J. Quinn, Appl. Phys. Lett. **2**, 167 (1963).
 - ⁴⁶ C. López-Bastidas, J. A. Maytorena, and A. Liebsch, Phys. Rev. B **65**, 35417 (2001).
 - ⁴⁷ E. V. Chulkov, V. M. Silkin, and P. M. Echenique, Surf. Sci. **391**, L1217 (1997); Surf. Sci. **437**, 330 (1999).
 - ⁴⁸ P. B. Johnson and R. W. Christy, Phys. Rev. B **6**, 4370 (1972).
 - ⁴⁹ V. P. Zhukov, F. Aryasetiawan, E. V. Chulkov, I. G. Gurtubay, and P. M. Echenique, Phys. Rev. B **64**, 195122 (2001).
 - ⁵⁰ A. Liebsch, Phys. Rev. Lett. **71**, 145 (1993); A. Liebsch, *Electronic Excitations at Metal Surfaces* (Plenum, New York, 1997).